

# Maternal Loss of *Ube3a* Produces an Excitatory/Inhibitory Imbalance through Neuron Type-Specific Synaptic Defects

Michael L. Wallace,<sup>1</sup> Alain C. Burette,<sup>2</sup> Richard J. Weinberg,<sup>2,3</sup> and Benjamin D. Philpot<sup>1,3,4,5,\*</sup>

<sup>1</sup>Curriculum in Neurobiology

<sup>2</sup>Department of Cell and Developmental Biology

<sup>3</sup>Neuroscience Center

<sup>4</sup>Carolina Institute for Developmental Disabilities

<sup>5</sup>Department of Cell and Molecular Physiology

University of North Carolina, Chapel Hill, NC 27599-7545, USA

\*Correspondence: bphilpot@med.unc.edu

DOI 10.1016/j.neuron.2012.03.036

## SUMMARY

Angelman syndrome (AS) is a neurodevelopmental disorder caused by loss of the maternally inherited allele of *UBE3A*. AS model mice, which carry a maternal *Ube3a* null mutation (*Ube3a<sup>m-/p+</sup>*), recapitulate major features of AS in humans, including enhanced seizure susceptibility. Excitatory neurotransmission onto neocortical pyramidal neurons is diminished in *Ube3a<sup>m-/p+</sup>* mice, seemingly at odds with enhanced seizure susceptibility. We show here that inhibitory drive onto neocortical pyramidal neurons is more severely decreased in *Ube3a<sup>m-/p+</sup>* mice. This inhibitory deficit follows the loss of excitatory inputs and appears to arise from defective presynaptic vesicle cycling in multiple interneuron populations. In contrast, excitatory and inhibitory synaptic inputs onto inhibitory interneurons are largely normal. Our results indicate that there are neuron type-specific synaptic deficits in *Ube3a<sup>m-/p+</sup>* mice despite the presence of *Ube3a* in all neurons. These deficits result in excitatory/inhibitory imbalance at cellular and circuit levels and may contribute to seizure susceptibility in AS.

## INTRODUCTION

Angelman syndrome (AS) is characterized by severe intellectual disabilities, EEG abnormalities, gait disturbances, disrupted sleep patterns, profound language impairment, and autism (Williams et al., 2006). Seizures are present in 90% of AS patients, significantly impacting their quality of life and that of their caregivers (Thibert et al., 2009). AS is caused by deletions or loss-of-function mutations in the maternally inherited allele of *UBE3A* (Rougeulle et al., 1997). *UBE3A* encodes an E3 ubiquitin ligase that, in the brain, is expressed primarily from the maternal allele as a result of neuron-specific imprinting (Albrecht

et al., 1997). Similar to humans with AS, mice lacking maternal *Ube3a* (*Ube3a<sup>m-/p+</sup>*) have abnormal EEG activity and are susceptible to cortical seizures, suggesting that loss of *Ube3a* might disrupt the excitatory/inhibitory balance in the neocortex (Jiang et al., 1998).

Loss of maternally inherited *Ube3a* results in decreased excitatory synaptic drive onto pyramidal neurons in layer 2/3 (L2/3) of neocortex, as evidenced by a loss of dendritic spines (Yashiro et al., 2009). Decreased *Ube3a*-mediated proteasomal degradation of Arc and Ephexin5 proteins may lead to excitatory synaptic defects (Greer et al., 2010; Margolis et al., 2010). These observations suggest a mechanism for how the loss of *Ube3a* may cause fewer and/or weaker excitatory synapses. While these deficits may be relevant to cognitive phenotypes in *Ube3a<sup>m-/p+</sup>* mice, they would not on their own predict hyperexcitability and increased seizure susceptibility. We hypothesized that *Ube3a* loss results in more severe inhibitory deficits, with the net outcome favoring cortical hyperexcitability.

Here, we use the visual cortex as a model to study the role of *Ube3a* in the establishment and function of inhibitory circuits. We show that *Ube3a<sup>m-/p+</sup>* mice have an abnormal accumulation of clathrin-coated vesicles at inhibitory axon terminals, indicating a defect in vesicle cycling. Consistent with this observation, inhibitory synaptic transmission onto L2/3 pyramidal neurons recovers slower following vesicle depletion in *Ube3a<sup>m-/p+</sup>* mice, compared to wild-types. Recovery following high-frequency stimulation of excitatory synapses onto L2/3 pyramidal neurons, however, is normal. This discrepancy among synapse types may further contribute to excitatory/inhibitory imbalance during high levels of activity. Finally, we show that synaptic inputs onto inhibitory neurons in *Ube3a<sup>m-/p+</sup>* mice are largely normal. We conclude that neuron type-specific synaptic deficits are likely to underlie neocortical excitatory/inhibitory imbalance in AS.

## RESULTS

### Inhibitory Deficits in Mature *Ube3a<sup>m-/p+</sup>* Mice

An excitatory/inhibitory imbalance in AS could arise from reduced numbers of inhibitory interneurons, abnormal inhibitory

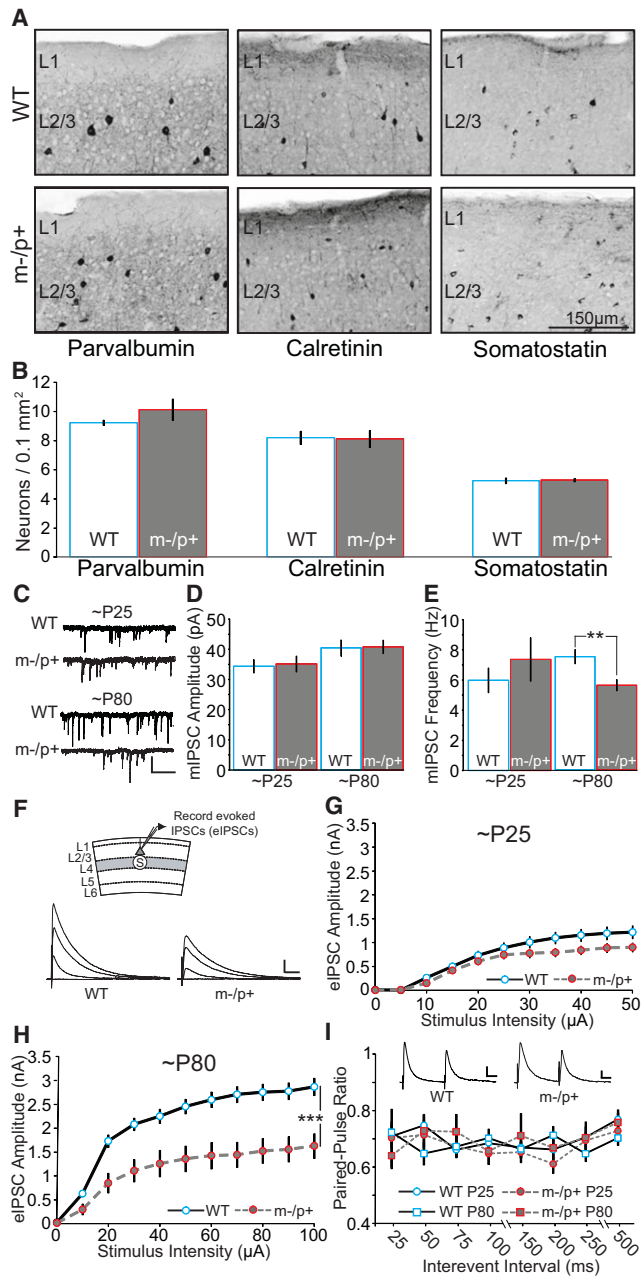


**Figure 1. Inhibitory Synaptic Deficits Arising through Development in *Ube3a*<sup>m-/p+</sup> Mice Are Not Due to Decreased Density of Inhibitory Interneurons**

(A) Photomicrographs showing immunocytochemical markers for inhibitory interneurons in visual cortex of wild-type (WT) and *Ube3a*-deficient (*m-/p+*) mice. (B) Quantification of parvalbumin-, calretinin-, and somatostatin-positive neurons in L2/3 of mouse primary visual cortex at ~P80 (n = 4 mice/genotype). (C) Sample mIPSC recordings from ~P25 (P21–P28) and ~P80 (P70–P90) WT and *Ube3a*<sup>m-/p+</sup> mice. Scale bar represents 30 pA, 400 ms. (D) Average mIPSC amplitude was similar between WT and *Ube3a*<sup>m-/p+</sup> mice at ~P25 (WT n = 10 cells; *m-/p+* n = 8 cells) and ~P80 (n = 13 cells/genotype) in L2/3 pyramidal cells. (E) Average mIPSC frequency for ~P25 (WT n = 10 cells; *m-/p+* n = 8 cells) and ~P80 (n = 13 cells/genotype). See also Table S1. (F) Illustration of stimulation (L4) and recording (L2/3 pyramidal neuron) configuration in primary visual cortex, and sample recordings of evoked IPSCs at stimulation intensities

connectivity, and/or decreased inhibitory neurotransmission. To test the first possibility, we performed immunohistochemistry for three markers—parvalbumin, calretinin, and somatostatin—which together label 96% of the total GABAergic interneurons in L2/3 of mouse primary visual cortex (V1) (Gonchar et al., 2007). We compared *Ube3a*<sup>m-/p+</sup> mice and their wild-type (WT) 129Sv/Ev strain littermate controls at postnatal day 80 (P80), an age where AS model mice exhibit abnormal EEG patterns and are susceptible to seizures (Jiang et al., 1998). We found no differences in the density of inhibitory interneurons expressing these markers (Figures 1A and 1B), implying that the relative number of inhibitory interneurons is normal in L2/3 of V1.

Next we investigated the strength and number of inhibitory synapses onto L2/3 pyramidal neurons. Using whole-cell voltage-clamp, we recorded miniature inhibitory postsynaptic currents (mIPSCs) in the presence of tetrodotoxin to gauge spontaneous inhibitory synaptic activity onto excitatory L2/3 pyramidal neurons. We recorded mIPSCs at two ages: P25, during the critical period for ocular dominance plasticity and when excitatory deficits have been observed previously, and P80, when the visual cortex is fully mature. We observed no difference in mIPSC amplitude between WT and *Ube3a*<sup>m-/p+</sup> mice at either P25 or P80, suggesting that the loss of *Ube3a* did not change the strength of inhibitory synapses (Figure 1D and Table S1 available online). While we saw no genotypic differences in mIPSC frequency at P25, L2/3 pyramidal neurons in *Ube3a*<sup>m-/p+</sup> mice had a reduction in mIPSC frequency by P80 (Figure 1E). These observations indicate that the loss of *Ube3a* leads to fewer functional inhibitory synapses, or a reduction of their release probability onto L2/3 pyramidal neurons.

To further investigate the development of inhibitory inputs onto L2/3 pyramidal neurons, we recorded evoked inhibitory postsynaptic currents (eIPSCs) using L4 stimulation at different intensities in P25 and P80 *Ube3a*<sup>m-/p+</sup> and WT mice (Figure 1F). This type of stimulation activates diverse inhibitory inputs and, with strong stimulation, can activate most of the inhibitory inputs onto L2/3 pyramidal neurons (Morales et al., 2002). We saw no significant difference in eIPSC amplitude at P25 (Figure 1G), but a large decrease in eIPSC amplitude at P80 in *Ube3a*<sup>m-/p+</sup> mice compared to WT (Figure 1H). Together, these results confirm that there is a severe deficit in the amount of inhibition arriving onto L2/3 pyramidal cells in the mature visual cortex of *Ube3a*<sup>m-/p+</sup> mice.

In principle, a decrease in eIPSC amplitude could arise from reductions in the number of postsynaptic GABA receptors, a decrease in the release probability of inhibitory axon terminals, fewer functional inhibitory synapses, or a depolarized inhibitory interneuron action potential threshold. It is unlikely that the decrease in eIPSC amplitude at P80 is due to a decrease in the number of GABA receptors at active synapses, since the

of 0, 10, 30, and 100 μA. Scale bar represents 500 pA, 30 ms. (G and H) Evoked IPSCs at ~P25 (WT n = 26 cells; *m-/p+* n = 29 cells) (G) and ~P80 (WT n = 20 cells; *m-/p+* n = 14 cells) (H). (I) Sample recordings of evoked IPSCs in paired-pulse experiments (scale bar represents 100 pA, 20 ms) and quantification of paired-pulse ratio in mice aged ~P25 (WT n = 12 cells; *m-/p+* n = 11 cells) and ~P80 (WT n = 13 cells; *m-/p+* n = 8 cells). All data are represented as the mean ± SEM; \*\*p < 0.01, \*\*\*p < 0.001. See also Figure S1.

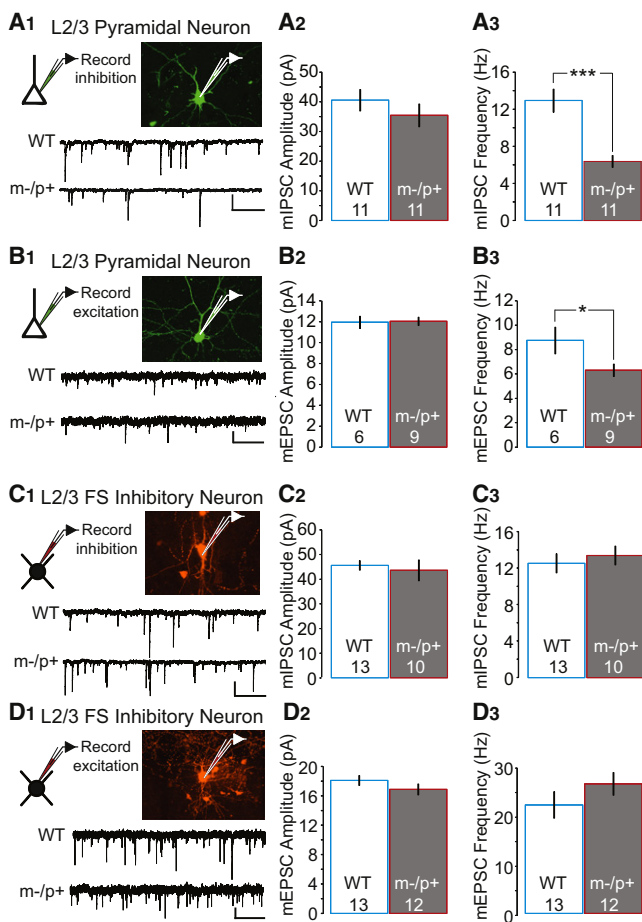


**Figure 2. Ube3a Loss Leads to Neuron Type-Specific Defects in Inhibitory Neurotransmission**

(A<sub>1</sub>) Illustration and photomicrograph of a filled L2/3 pyramidal neuron and sample recordings from ~P80 WT (upper) and *Ube3a*<sup>m-/p+</sup> (lower) mice. Scale bar represents 40 pA, 300 ms. (A<sub>2</sub> and A<sub>3</sub>) Average mIPSC amplitude (n = 11 cells/genotype, p = 0.16) (A<sub>2</sub>) and frequency (n = 11 cells/genotype) from L2/3 pyramidal neurons (A<sub>3</sub>). (B<sub>1</sub>) Illustration and fill of a L2/3 pyramidal neuron and sample recordings from ~P80 WT (upper) and *Ube3a*<sup>m-/p+</sup> (lower) mice. Scale bar represents 15 pA, 300 ms. (B<sub>2</sub>) Average mEPSC amplitude (WT n = 6 cells; m-/p+ n = 9 cells) and (B<sub>3</sub>) frequency (WT n = 6 cells; m-/p+ n = 9 cells) from L2/3 pyramidal neurons. (C<sub>1</sub>) Illustration and fill of a L2/3 FS inhibitory interneuron and sample recordings from ~P80 WT (upper) and *Ube3a*<sup>m-/p+</sup> (lower) mice. Scale bar represents 40 pA, 300 ms. (C<sub>2</sub> and C<sub>3</sub>) Average mIPSC amplitude (WT n = 13 cells; m-/p+ n = 10 cells) (C<sub>2</sub>) and frequency (WT n = 13 cells; m-/p+ n = 10 cells; p = 0.57) (C<sub>3</sub>) from L2/3 FS inhibitory interneurons. (D<sub>1</sub>) Illustration and fill of a L2/3 FS inhibitory interneuron and sample recordings from ~P80 WT (upper) and *Ube3a*<sup>m-/p+</sup> (lower) mice. Scale bar represents 10 pA, 300 ms. (D<sub>2</sub> and D<sub>3</sub>) Average mEPSC amplitude (WT n = 13 cells; m-/p+ n = 12 cells) (D<sub>2</sub>) and frequency (WT n = 13 cells; m-/p+ n = 12 cells) (D<sub>3</sub>) from L2/3 FS inhibitory interneurons. Bar graphs represent the mean ± SEM; p < 0.05, p\*\*\* < 0.001. See also Figure S2 and Table S2.

amplitude of mIPSCs was similar in *Ube3a*<sup>m-/p+</sup> and WT mice. To assess whether the decrease in eIPSC amplitude is due to the loss of functional synapses or to a decrease in release probability, we examined the paired-pulse ratio of inhibitory inputs.

Specifically, we stimulated L4 at varying interpulse intervals to evoke IPSCs in L2/3 pyramidal cells, and compared the paired-pulse ratio in WT and *Ube3a*<sup>m-/p+</sup> mice. We observed no difference in the paired-pulse ratio between genotypes at either P25 or P80, implying that release at functional inhibitory inputs onto L2/3 pyramidal cells is normal in response to brief stimuli given at several interpulse intervals (Figure 1I). Finally, we found no difference in the action potential threshold or intrinsic excitability of FS neurons (a major class of inhibitory interneurons) in *Ube3a*<sup>m-/p+</sup> mice compared to WT, indicating that reduced eIPSC amplitude is unlikely to be due to reductions in evoked action potentials in inhibitory interneurons (Figures S1A and S1B). By exclusion, our data suggest a reduction in the total number of functional inhibitory synapses.

### Neuron Type-Specific Reduction in Functional Synapses in *Ube3a*<sup>m-/p+</sup> Mice

Our previous observations of reduced inhibition were made in *Ube3a*<sup>m-/p+</sup> mice on the 129Sv/Ev strain, which are susceptible to spontaneous seizures (Jiang et al., 1998), making it difficult to determine whether the synaptic abnormalities were a cause or result of seizures (Sloviter, 1987). To address this concern, we tested for possible synaptic deficits in *Ube3a*<sup>m-/p+</sup> mice maintained on the C57BL/6J strain, which have a low incidence of evoked seizures and no reported spontaneous seizures (Jiang et al., 1998). We performed mIPSC recordings at P80 in WT and *Ube3a*<sup>m-/p+</sup> C57BL/6J mice to test if synaptic defects arose in the absence of spontaneous seizures. As before, we observed no genotypic differences in the amplitude of mIPSCs, but a large decrease in mIPSC frequency in *Ube3a*<sup>m-/p+</sup> mice (Figure 2A). We also performed mEPSC recordings in L2/3 pyramidal neurons in mice on the C57BL/6J strain to confirm previous results from the 129Sv/Ev strain (Yashiro et al., 2009). Consistent with previous results, there was a significant decrease in mEPSC frequency, but not amplitude, between *Ube3a*<sup>m-/p+</sup> and WT mice (Figure 2B). These observations reveal that *Ube3a*<sup>m-/p+</sup> L2/3 pyramidal neurons have a 50% reduction in spontaneous inhibitory synaptic activity, but only a 28% decrease in excitatory synaptic activity. Additionally, intrinsic excitability of L2/3 pyramidal neurons was increased in *Ube3a*<sup>m-/p+</sup> mice compared to WT (Figure S1C). Together these data suggest that a disproportionate loss of inhibition may lead to an excitatory/inhibitory imbalance in *Ube3a*<sup>m-/p+</sup> L2/3 pyramidal neurons.

*Ube3a* is expressed by both excitatory and inhibitory interneurons in the cerebral cortex (Sato and Stryker, 2010). Therefore, *Ube3a* loss might be expected to affect both neuron classes. To assess this possibility, we recorded spontaneous synaptic activity in fast-spiking (FS) inhibitory interneurons, which we identified by membrane properties, aspiny dendrites, and characteristic high firing rates (Okaty et al., 2009). FS inhibitory interneurons in L2/3 were targeted for whole-cell recording at P80, an age at which excitatory and inhibitory neurotransmission onto L2/3 pyramidal neurons is altered. In contrast to L2/3 pyramidal neurons, the loss of *Ube3a* did not affect either the amplitude or the frequency of mIPSCs onto FS inhibitory interneurons (Figure 2C). Moreover, excitatory connections onto FS inhibitory interneurons appeared normal, as *Ube3a* loss did not alter mEPSC amplitude or frequency (Figure 2D).

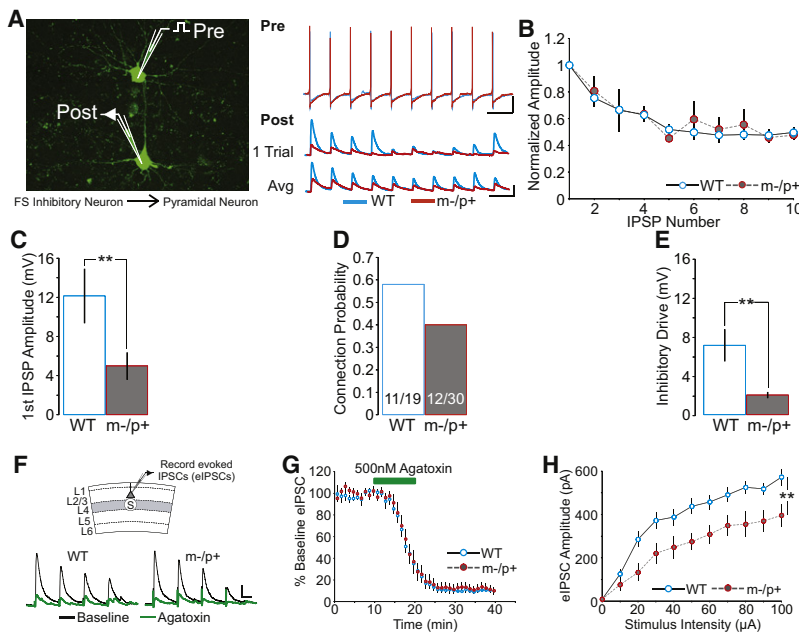


**Figure 3. Synaptic Deficits Arise from Both FS and Non-FS Inhibitory Interneurons in *Ube3a*<sup>m-/p+</sup> Mice**

(A) Recording configuration (upper) and representative recordings of presynaptic action potentials evoked in a FS inhibitory interneuron (middle), and resulting unitary IPSPs in a L2/3 pyramidal neuron (lower) from WT (blue) and *Ube3a*<sup>m-/p+</sup> mice (red). Average is of 12 trials. Scale bar represents 20mV (“Pre”), 40 ms; 4mV (“Post”), 40 ms. (B) Average short-term plasticity of inhibitory to excitatory connections (WT n = 8; m-/p+ n = 12) (presynaptic spikes at 30 Hz). (C) Average unitary IPSP amplitude of 1<sup>st</sup> IPSP of inhibitory to excitatory connections (WT n = 8; m-/p+ n = 12). (D and E) Connection probability of FS inhibitory interneurons to L2/3 pyramidal neurons (numbers of connected/total pairs written in bars) (D); inhibitory drive of FS inhibitory interneurons to L2/3 pyramidal neurons (WT n = 19 pairs; m-/p+ n = 30 pairs) (E). (F) Recording configuration (upper) and representative recordings (lower) of eIPSCs during baseline (black) and 20 min after 500 nM ω-agatoxin-IVa perfusion (green). Scale bar represents 100 pA, 20 ms. (G) A 10 min baseline was recorded before a 10 min perfusion of agatoxin (green bar) (WT n = 10; m-/p+ n = 10). (H) Input-output relationship in the agatoxin-insensitive portion of total eIPSC performed 20 min after cessation of agatoxin perfusion (WT n = 10; m-/p+ n = 10). Data are represented as the mean ± SEM; \*p < 0.05, \*\*p < 0.01, \*\*\*p < 0.001. See also Figure S3 and Table S3.

Similar to L2/3, *Ube3a* loss did not change the frequency or amplitude of mIPSCs or mEPSCs onto L5/6 FS inhibitory interneurons (Figures S2A and S2B). These results imply that *Ube3a* loss has neuron type-specific synaptic effects.

***Ube3a* Loss Results in Inhibitory Deficits from FS Interneurons**

We examined the effects of *Ube3a* loss on FS inhibitory interneurons, which provide the majority of perisomatic inhibitory input to L2/3 pyramidal neurons (Jiang et al., 2010), impart feed-forward and feedback inhibition, and have been implicated in seizure susceptibility (Di Cristo et al., 2004). Despite the challenge of performing paired recordings in adult neocortical slices, we were able to investigate synaptic connectivity between 83 pairs of L2/3 FS inhibitory interneurons and L2/3 pyramidal neurons in WT and *Ube3a*<sup>m-/p+</sup> mice at P80 (Table S3).

We first analyzed synaptic connectivity from FS inhibitory interneurons to pyramidal neurons. Using current-clamp recordings, we evoked action potentials in FS interneurons with depolarizing current injections at 30 Hz, and simultaneously recorded the response in pyramidal neurons (Figure 3A). To measure short-term plasticity we normalized the amplitude of the evoked IPSPs to the amplitude of the first IPSP in the train. We observed no change in the short-term plasticity between genotypes (Figure 3B). However, the amplitude of the first IPSP between these pairs was significantly decreased in *Ube3a*<sup>m-/p+</sup> mice, indicating decreased connection strength from FS inhibitory interneurons to L2/3 pyramidal neurons (Figure 3C). We also found a 31% decrease in connection probability in *Ube3a*<sup>m-/p+</sup> mice compared to WT mice (Figure 3D), supporting the conclusion that the decreased IPSP amplitude is likely due to a reduction in the number of functional synapses made from

FS interneurons to pyramidal neurons. Finally, we estimated the average inhibitory drive from FS inhibitory interneurons onto L2/3 pyramidal neurons, by calculating the product of connection strength and connection probability, finding that inhibitory drive was reduced by 71% in *Ube3a*<sup>m-/p+</sup> mice compared to WT mice (Figure 3E).

To further investigate possible effects of *Ube3a* loss on synaptic connectivity, we examined the connections from L2/3 pyramidal neurons to FS inhibitory interneurons. We measured short-term plasticity and found that *Ube3a*<sup>m-/p+</sup> mice had increased facilitation at synapses from pyramidal neuron to FS interneurons (Figure S3B). To assess connection strength in this pathway, we measured the amplitude of the first EPSP evoked in the postsynaptic FS interneuron, detecting no difference between genotypes (Figure S3C). Finally, we found no genotypic difference in the connection probability of L2/3 pyramidal to FS inhibitory interneuron pairs (Figure S3D).

These data suggest that, while excitatory connection frequency and strength onto L2/3 FS interneurons are unchanged in *Ube3a*<sup>m-/p+</sup> mice, excitatory inputs onto FS inhibitory interneurons have altered short-term plasticity, potentially leading to defective engagement of FS inhibitory interneurons during trains of activity. The unchanged strength of the pyramidal-to-FS inhibitory interneuron connections in *Ube3a*<sup>m-/p+</sup> mice was unexpected, since short-term plasticity measurements indicated a change in release probability at this synapse. We conclude that other factors, such as differences in calcium buffering, coupling of calcium channels to release machinery, or vesicular trafficking, must underlie the observed changes (Atwood and Karunanithi, 2002). Together, these experiments identify a specific inhibitory interneuron subtype, FS inhibitory interneurons, that is at least partially responsible for the

decrease in inhibition found in L2/3 pyramidal neurons in the AS model.

### Ube3a Loss Results in Inhibitory Deficits from Non-FS Interneurons

L2/3 pyramidal neurons receive inhibition from a variety of inhibitory interneuron subtypes (Markram et al., 2004). To test whether inhibitory deficits in *Ube3a*<sup>m-/-p+</sup> mice could also be ascribed to other types of interneurons, we used agatoxin, a potent irreversible antagonist of P/Q-type voltage-gated calcium channels (VGCCs), to block release of GABA selectively from FS inhibitory interneurons (Jiang et al., 2010). Agatoxin suppressed ~90% of the total eIPSCs in both WT and *Ube3a*<sup>m-/-p+</sup> mice 20 min after perfusion of the toxin (Figure 3G). The agatoxin-insensitive portion of the eIPSC had an increased latency from stimulation onset and an increased rise time, suggesting that the agatoxin-insensitive inputs targeted the distal dendrites of L2/3 pyramidal neurons (Figures S3G and S3H). Agatoxin-insensitive inputs also had decreased paired-pulse depression compared to the total eIPSC, a signature of non-FS inhibitory interneurons (Figure S3F) (Gupta et al., 2000). After agatoxin perfusion, we recorded eIPSCs at different stimulation intensities and again found a decrease in the strength of inhibitory inputs in the *Ube3a*<sup>m-/-p+</sup> mice, compared to WT, demonstrating that Ube3a loss also affects inputs from non-FS classes of inhibitory interneurons (Figure 3H).

### Ube3a<sup>m-/-p+</sup> Mice Have Defects in Synaptic Vesicle Cycling

Our electrophysiological data suggest that inhibitory deficits in *Ube3a*<sup>m-/-p+</sup> mice result from a loss of functional inhibitory synapses onto L2/3 pyramidal neurons. However, a reduction in functional synapses could arise anatomically from fewer synaptic contacts, postsynaptically by a loss of functional receptors, or presynaptically by a severe depletion of releasable synaptic vesicles rendering a subset of inhibitory axon terminals nonfunctional. To test for an anatomical correlate to our functional data, we used immunohistochemistry to stain WT and *Ube3a*<sup>m-/-p+</sup> mice for the vesicular GABA transporter (VGAT), a marker for the axon terminals of inhibitory interneurons (Chaudhry et al., 1998). We were surprised to see similar densities of VGAT-positive puncta in WT and *Ube3a*<sup>m-/-p+</sup> mice, suggesting no change in the number of inhibitory interneuron axon terminals (Figures S4A–S4C). However, there remained the possibility that some of these axon terminals were nonfunctional. To explore this possibility, we used electron microscopy to examine synaptic structure in WT and *Ube3a*<sup>m-/-p+</sup> mice. Post-embedding immunogold localization of GABA was used to identify inhibitory synapses onto somata in L2/3 of V1. The area of GABA-positive axon terminals and proportion of mitochondria per terminal were not different between WT and *Ube3a*<sup>m-/-p+</sup> mice (Figures 4A<sub>2</sub> and 4A<sub>3</sub>). However, there was a decrease in the number of synaptic vesicles, and a large increase in the number of clathrin-coated vesicles (CCVs), in the *Ube3a*<sup>m-/-p+</sup> mice compared to WT (Figures 4A<sub>4</sub> and 4A<sub>5</sub> and S4F and S4G). We also tested whether the defects we observed in inhibitory synapses were generalized to excitatory synapses. Similar to inhibitory synapses, we observed a decrease in the

number of synaptic vesicles, but no change in the area of excitatory axon terminals or the proportion of mitochondria per terminal (Figures 4B<sub>1</sub>–4B<sub>4</sub> and S4D and S4E). Finally, we saw little or no decrease in the number of CCVs at excitatory synapses between genotypes (Figures 4B<sub>5</sub> and S4D and S4E). These data suggest a defect in synaptic vesicle cycling in inhibitory synapses of *Ube3a*<sup>m-/-p+</sup> mice.

### Incomplete Recovery of IPSCs after High-Frequency Stimulation in Ube3a<sup>m-/-p+</sup> Mice

Previous studies examining synaptic vesicle cycling have identified genes whose mutation leads to increased numbers of CCVs in axon terminals (Slepnev and De Camilli, 2000). Many of these mutant synapses maintain the ability to release neurotransmitter and have normal short-term plasticity; however, during periods of high activity these synapses fail to adequately replenish their synaptic vesicle pool, resulting in a delayed recovery to baseline levels of transmitter release (Luthi et al., 2001). These studies led us to test whether inhibitory synapses in the *Ube3a*<sup>m-/-p+</sup> mice had functional deficits similar to other synaptic vesicle cycling mutants. We applied a train of 800 stimuli at 10 Hz while recording eIPSCs in L2/3 pyramidal neurons in WT and *Ube3a*<sup>m-/-p+</sup> mice (Figure 4C). We then decreased the stimulation frequency to 0.33 Hz and recorded the recovery phase of the eIPSC (Figure 4C<sub>1</sub>). Ube3a loss had no effect on the depletion phase of the eIPSC (Figure 2C<sub>2</sub>) in agreement with our previous experiments examining short-term plasticity (Figures 1I and 3B). However, we found a large decrease in the rate and level of recovery of the eIPSC in *Ube3a*<sup>m-/-p+</sup> mice compared to WT (Figure 4C<sub>3</sub>). These data are consistent with defects in inhibitory synaptic vesicle cycling in *Ube3a*<sup>m-/-p+</sup> mice. Specifically, the decrease in recovery of the eIPSC, combined with the increase in CCVs, suggests an inability of newly endocytosed CCVs to reenter and replenish the synaptic vesicle pool. These defects may render a subset of inhibitory synapses nonfunctional in *Ube3a*<sup>m-/-p+</sup> mice.

Finally, we challenged excitatory synapses with the same high frequency stimulation protocol that we used to test inhibitory synapses (Figure 4D<sub>1</sub>). Unlike inhibitory synapses, Ube3a loss did not have an effect on the recovery of excitatory synapses from high-frequency stimulation (Figure 4D<sub>3</sub>). Thus, the pronounced accumulation of CCVs observed at inhibitory synapses correlates well with the selective deficits in the synaptic recovery from high-frequency stimulation. Moreover, these functional data demonstrate that a period of heightened excitatory/inhibitory imbalance may occur following a high-frequency train of activity in this circuit.

## DISCUSSION

This work demonstrates that maternal loss of *Ube3a*, as seen in individuals with AS, leads to neuron type-specific synaptic deficits. Our findings suggest that loss of Ube3a can result in an excitatory/inhibitory imbalance in the neocortex.

Earlier studies showing decreased excitatory neurotransmission in *Ube3a*<sup>m-/-p+</sup> mice were difficult to reconcile with reports of high seizure susceptibility (Jiang et al., 1998; Yashiro et al., 2009). Our data provides clarification, showing that the loss of

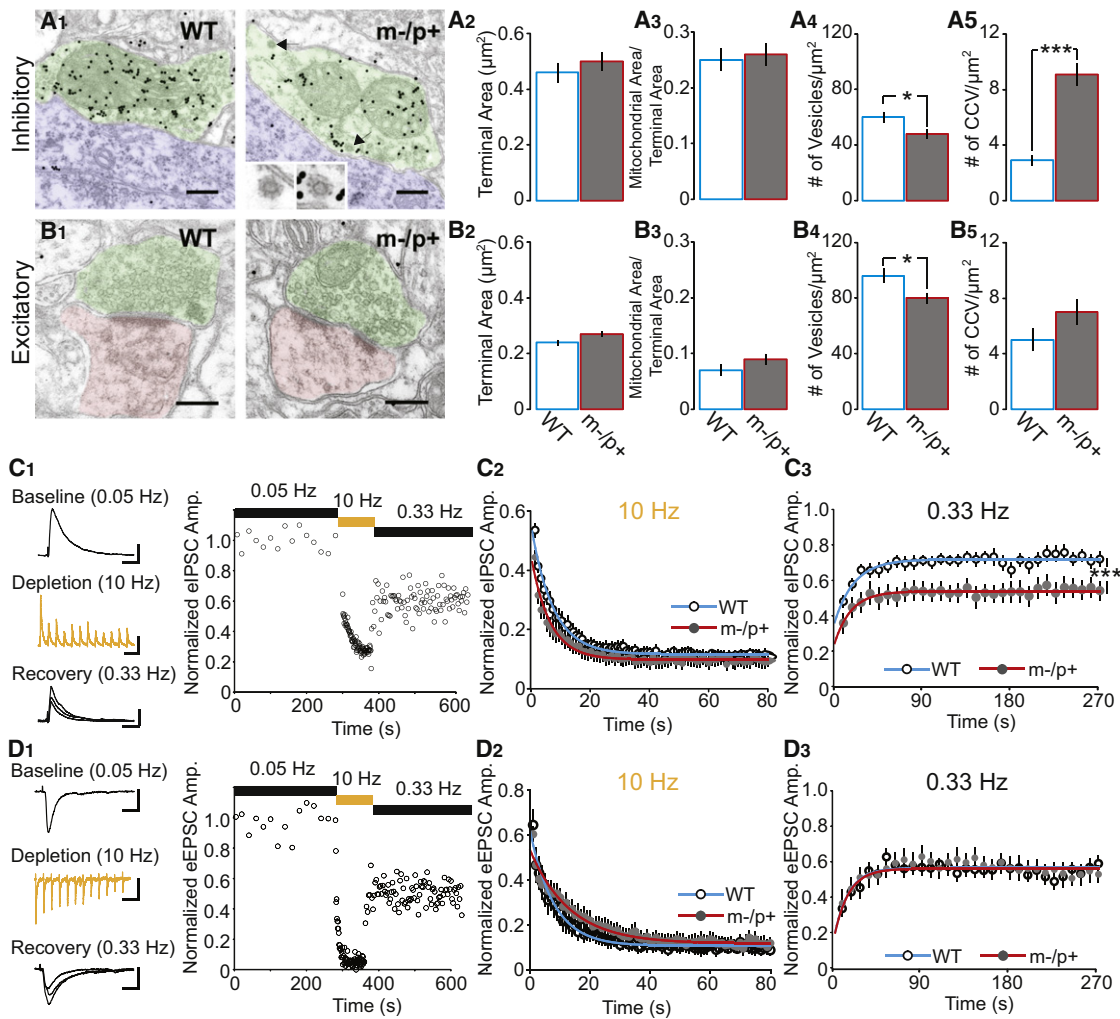


**Figure 4. Inhibitory Synapses of *Ube3a*<sup>m-/p+</sup> Mice Have Presynaptic Defects**

(A<sub>1</sub>) Electron micrographs of inhibitory synapses stained for GABA in ~P80 WT and *Ube3a*<sup>m-/p+</sup> mice (green denotes axon terminal, blue denotes soma), insets highlight CCVs. Scale bar represents 250 nm. Average values of (left to right) (A<sub>2</sub>) axon terminal area, (A<sub>3</sub>) mitochondrial area divided by terminal area, (A<sub>4</sub>) number of synaptic vesicles per  $\mu\text{m}^2$ , and (A<sub>5</sub>) number of CCVs per  $\mu\text{m}^2$  (WT n = 3; m-/p+ n = 4). (B<sub>1</sub>) Electron micrographs of excitatory synapses in WT and *Ube3a*<sup>m-/p+</sup> mice (green denotes axon terminal, red denotes spine). Scale bar represents 250 nm. Average values of (left to right) (B<sub>2</sub>) axon terminal area, (B<sub>3</sub>) mitochondrial area divided by terminal area, (B<sub>4</sub>) number of synaptic vesicles per  $\mu\text{m}^2$ , and (B<sub>5</sub>) number of CCVs per  $\mu\text{m}^2$  (WT n = 3; m-/p+ n = 4). (C<sub>1</sub>) Sample recordings (left) and sample experiment (right) showing baseline (black), high frequency depletion (orange), and recovery (black) phases. Scale bars represent baseline = 200 pA, 20 ms; depletion = 200 pA, 200 ms; recovery = 200 pA, 20 ms. (C<sub>2</sub>) Average depletion phase showing eIPSC amplitude normalized to baseline during 800 stimuli at 10 Hz. Ten responses are averaged for each point and a monophasic exponential was fit to the averaged responses for WT and *Ube3a*<sup>m-/p+</sup> mice (WT n = 19; m-/p+ n = 18). (C<sub>3</sub>) Average recovery phase showing eIPSC amplitude normalized to baseline during 90 stimuli at 0.33 Hz. Three responses are averaged for each point and a monophasic exponential was fit to the averaged responses for WT and *Ube3a*<sup>m-/p+</sup> mice (WT n = 19; m-/p+ n = 18). (D<sub>1</sub>) Sample recordings (left) and sample experiment (right) showing baseline (black), high frequency depletion (orange), and recovery (black) phases. Scale bars represent baseline = 100 pA, 10 ms; depletion = 100 pA, 200 ms; recovery = 100 pA, 10 ms. (D<sub>2</sub>) Average depletion phase showing eEPSC amplitude normalized to baseline during 800 stimuli at 10 Hz. Ten responses are averaged for each point and a monophasic exponential was fit to the averaged responses for WT and *Ube3a*<sup>m-/p+</sup> mice (WT n = 10; m-/p+ n = 11). (D<sub>3</sub>) Average recovery phase showing eEPSC amplitude normalized to baseline during 90 stimuli at 0.33 Hz. Three responses are averaged for each point and a monophasic exponential was fit to the averaged responses for WT and *Ube3a*<sup>m-/p+</sup> mice (WT n = 10; m-/p+ n = 11). Data are represented as the mean  $\pm$  SEM; \*p < 0.05, \*\*\*p < 0.001.

See also Figure S4.

*Ube3a* causes a particularly severe decrease in inhibitory input to L2/3 pyramidal neurons. We also report that AS model mice have a synaptic vesicle cycling defect, which suggests a basis for this deficit. The vesicle cycling defects we observe are similar to those observed after deletion of the presynaptic proteins

synaptojanin (Cremona et al., 1999) or endophilin (Milosevic et al., 2011), both which lead to increased CCVs at synaptic terminals, and decreased synaptic recovery from high levels of activity. Notably, inhibitory synapses may be particularly sensitive to disruptions in vesicular trafficking, due to their enhanced

activity and smaller vesicle pools (Hayashi et al., 2008). These results, combined with our functional studies describing defective inhibitory synaptic transmission in *Ube3a<sup>m-/-p+</sup>* mice, suggest a means by which a hyperexcitable cortical circuit could arise despite fewer excitatory synapses.

Ube3a is present in both excitatory and inhibitory interneurons in the brain (Sato and Stryker, 2010). Our results showing different synaptic defects onto excitatory and inhibitory neurons indicate Ube3a deficiency causes neuron type-specific deficits. Since Ube3a targets its substrate proteins for proteasomal degradation, the consequences of Ube3a loss may depend on which substrate proteins are normally present in a cell. This hypothesis is supported by recent work showing that Arc, a protein expressed postsynaptically in excitatory but not inhibitory interneurons, is a Ube3a substrate (Greer et al., 2010; McCurry et al., 2010). Thus, the loss of Ube3a is expected to cause an inappropriate overexpression of Arc in excitatory neurons without affecting inhibitory interneurons. Given the ability of Arc to influence AMPA receptor endocytosis (Chowdhury et al., 2006), the neuron type-specific expression of Arc could partly explain the excitatory synaptic defects observed onto L2/3 pyramidal neurons and the lack of effect in FS interneurons. Conversely, our findings suggest a synaptic defect in *Ube3a<sup>m-/-p+</sup>* mice at inhibitory synapses, primarily affecting presynaptic function at inhibitory synapses and resulting in fewer functional synapses. Intriguingly, the observed excitatory and inhibitory defects both involve endocytic processes, albeit at different sides of the synaptic cleft, suggesting that common processes may be involved.

Altered function of GABA receptors and/or inhibitory interneurons has been hypothesized to underlie many of the phenotypes seen in AS (Dan and Boyd, 2003). While attention has focused on how defects in GABAergic neurotransmission may relate to epileptic phenotypes in AS, abnormalities in inhibition can have wide-ranging consequences, including disrupting synaptic plasticity, cortical network oscillations, and cortical circuit architecture (Cardin et al., 2009; Hensch, 2005). For example, FS inhibitory interneurons have a critical role in ocular dominance plasticity (Hensch et al., 1998), which is severely reduced in *Ube3a<sup>m-/-p+</sup>* mice (Sato and Stryker, 2010; Yashiro et al., 2009). Our finding that inhibitory interneuron to L2/3 pyramidal neuron connections are altered in *Ube3a<sup>m-/-p+</sup>* mice may prove important for understanding the mechanisms underlying plasticity and learning defects in AS. Understanding the specific synaptic impairments caused by the global loss of Ube3a may provide insights into the intractable nature of seizures found in many individuals with AS.

Excitatory/inhibitory imbalance has been observed in several genetic disorders that meet diagnostic criteria for autism spectrum disorders, including neuroligin-3 mutation, Fragile X, and Rett syndrome (Dani et al., 2005; Gibson et al., 2008; Tabuchi et al., 2007). Moreover, excitatory/inhibitory imbalance may be a general neurophysiological feature of autism spectrum disorders, contributing to inappropriate detection or integration of salient sensory information due to a decreased signal-to-noise ratio (Rubenstein and Merzenich, 2003). Our finding that an excitatory/inhibitory imbalance may develop in AS due to the loss of functional inhibitory synapses highlights

the importance of identifying Ube3a substrates in inhibitory interneurons.

## EXPERIMENTAL PROCEDURES

See Supplemental Experimental Procedures for details relating to electrophysiology and immunohistochemistry.

### Animals

*Ube3a*-deficient mice on the 129Sv/Ev background were originally developed by Jiang et al. (1998) and obtained through the Jackson Laboratory (Bar Harbor, ME). *Ube3a*-deficient mice backcrossed onto the C57BL/6J background were obtained from Yong-hui Jiang (Duke University) and crossed with mice expressing GFP in a subset of FS inhibitory neurons (Chattopadhyaya et al., 2004) obtained through Jackson Laboratory. All studies were conducted with protocols approved by the University of North Carolina at Chapel Hill Animal Care and Use Committee.

### Statistics

Most experiments and analyses were performed blind to genotype. Unpaired Student's *t* tests were used on all data excluding the following; input-output, frequency-current, short-term plasticity, connection probability, and for depletion and recovery experiments. Graphs represent the mean and error bars represent the SEM. For all figures *p*-values are as follows \**p* < 0.05, \*\**p* < 0.01, \*\*\**p* < 0.001. All statistics were performed in Graphpad Prism.

## SUPPLEMENTAL INFORMATION

Supplemental Information includes four figures, three tables, and Supplemental Experimental Procedures and can be found with this article online at doi:10.1016/j.neuron.2012.03.036.

## ACKNOWLEDGMENTS

We thank Rylan Larsen and Matt Judson for critical readings of the manuscript, Paul Manis for experimental advice, Yong-hui Jiang for his generous donation of C57BL/6J *Ube3a*-deficient mutant mice and Kristen Phend for histological support. Imaging was supported by the Confocal and Multiphoton Imaging Core of NINDS Center Grant P30 NS045892 and NICHD Center Grant P30 HD03110. M.L.W. was supported by a Neurobiology Research Training Grant from NINDS (5T32NS007431) and a National Research Service Award from NINDS (1F31NS077847). R.J.W. was supported by NINDS (5R01NS035527). B.D.P. was supported by the Angelman Syndrome Foundation, the Simons Foundation, the National Eye Institute (R01EY018323), and the National Institute of Mental Health (1R01MH093372).

Accepted: March 28, 2012

Published: June 6, 2012

## REFERENCES

- Albrecht, U., Sutcliffe, J.S., Cattanach, B.M., Beechey, C.V., Armstrong, D., Eichele, G., and Beaudet, A.L. (1997). Imprinted expression of the murine Angelman syndrome gene, *Ube3a*, in hippocampal and Purkinje neurons. *Nat. Genet.* 17, 75–78.
- Atwood, H.L., and Karunaniithi, S. (2002). Diversification of synaptic strength: presynaptic elements. *Nat. Rev. Neurosci.* 3, 497–516.
- Cardin, J.A., Carlén, M., Meletis, K., Knoblich, U., Zhang, F., Deisseroth, K., Tsai, L.H., and Moore, C.I. (2009). Driving fast-spiking cells induces gamma rhythm and controls sensory responses. *Nature* 459, 663–667.
- Chattopadhyaya, B., Di Cristo, G., Higashiyama, H., Knott, G.W., Kuhlman, S.J., Welker, E., and Huang, Z.J. (2004). Experience and activity-dependent maturation of perisomatic GABAergic innervation in primary visual cortex during a postnatal critical period. *J. Neurosci.* 24, 9598–9611.

- Chaudhry, F.A., Reimer, R.J., Bellocchio, E.E., Danbolt, N.C., Osen, K.K., Edwards, R.H., and Storm-Mathisen, J. (1998). The vesicular GABA transporter, VGAT, localizes to synaptic vesicles in sets of glycinergic as well as GABAergic neurons. *J. Neurosci.* *18*, 9733–9750.
- Chowdhury, S., Shepherd, J.D., Okuno, H., Lyford, G., Petralia, R.S., Plath, N., Kuhl, D., Huganir, R.L., and Worley, P.F. (2006). Arc/Arg3.1 interacts with the endocytic machinery to regulate AMPA receptor trafficking. *Neuron* *52*, 445–459.
- Cremona, O., Di Paolo, G., Wenk, M.R., Lüthi, A., Kim, W.T., Takei, K., Daniell, L., Nemoto, Y., Shears, S.B., Flavell, R.A., et al. (1999). Essential role of phosphoinositide metabolism in synaptic vesicle recycling. *Cell* *99*, 179–188.
- Dan, B., and Boyd, S.G. (2003). Angelman syndrome reviewed from a neurophysiological perspective. The UBE3A-GABRB3 hypothesis. *Neuropediatrics* *34*, 169–176.
- Dani, V.S., Chang, Q., Maffei, A., Turrigiano, G.G., Jaenisch, R., and Nelson, S.B. (2005). Reduced cortical activity due to a shift in the balance between excitation and inhibition in a mouse model of Rett syndrome. *Proc. Natl. Acad. Sci. USA* *102*, 12560–12565.
- Di Cristo, G., Wu, C., Chattopadhyaya, B., Ango, F., Knott, G., Welker, E., Svoboda, K., and Huang, Z.J. (2004). Subcellular domain-restricted GABAergic innervation in primary visual cortex in the absence of sensory and thalamic inputs. *Nat. Neurosci.* *7*, 1184–1186.
- Gibson, J.R., Bartley, A.F., Hays, S.A., and Huber, K.M. (2008). Imbalance of neocortical excitation and inhibition and altered UP states reflect network hyperexcitability in the mouse model of fragile X syndrome. *J. Neurophysiol.* *100*, 2615–2626.
- Gonchar, Y., Wang, Q., and Burkhalter, A. (2007). Multiple distinct subtypes of GABAergic neurons in mouse visual cortex identified by triple immunostaining. *Front Neuroanat* *1*, 3.
- Greer, P.L., Hanayama, R., Bloodgood, B.L., Mardinly, A.R., Lipton, D.M., Flavell, S.W., Kim, T.K., Griffith, E.C., Waldon, Z., Maehr, R., et al. (2010). The Angelman Syndrome protein Ube3A regulates synapse development by ubiquitinating arc. *Cell* *140*, 704–716.
- Gupta, A., Wang, Y., and Markram, H. (2000). Organizing principles for a diversity of GABAergic interneurons and synapses in the neocortex. *Science* *287*, 273–278.
- Hayashi, M., Raimondi, A., O'Toole, E., Paradise, S., Collesi, C., Cremona, O., Ferguson, S.M., and De Camilli, P. (2008). Cell- and stimulus-dependent heterogeneity of synaptic vesicle endocytic recycling mechanisms revealed by studies of dynamin 1-null neurons. *Proc. Natl. Acad. Sci. USA* *105*, 2175–2180.
- Hensch, T.K. (2005). Critical period plasticity in local cortical circuits. *Nat. Rev. Neurosci.* *6*, 877–888.
- Hensch, T.K., Fagiolini, M., Mataga, N., Stryker, M.P., Baekkeskov, S., and Kash, S.F. (1998). Local GABA circuit control of experience-dependent plasticity in developing visual cortex. *Science* *282*, 1504–1508.
- Jiang, B., Huang, S., de Pasquale, R., Millman, D., Song, L., Lee, H.K., Tsumoto, T., and Kirkwood, A. (2010). The maturation of GABAergic transmission in visual cortex requires endocannabinoid-mediated LTD of inhibitory inputs during a critical period. *Neuron* *66*, 248–259.
- Jiang, Y.H., Armstrong, D., Albrecht, U., Atkins, C.M., Noebels, J.L., Eichele, G., Sweatt, J.D., and Beaudet, A.L. (1998). Mutation of the Angelman ubiquitin ligase in mice causes increased cytoplasmic p53 and deficits of contextual learning and long-term potentiation. *Neuron* *21*, 799–811.
- Luthi, A., Di Paolo, G., Cremona, O., Daniell, L., De Camilli, P., and McCormick, D.A. (2001). Synaptotagmin 1 contributes to maintaining the stability of GABAergic transmission in primary cultures of cortical neurons. *J. Neurosci.* *21*, 9101–9111.
- Margolis, S.S., Salogiannis, J., Lipton, D.M., Mandel-Brehm, C., Wills, Z.P., Mardinly, A.R., Hu, L., Greer, P.L., Bikoff, J.B., Ho, H.Y., et al. (2010). EphB-mediated degradation of the RhoA GEF Ephexin5 relieves a developmental brake on excitatory synapse formation. *Cell* *143*, 442–455.
- Markram, H., Toledo-Rodriguez, M., Wang, Y., Gupta, A., Silberberg, G., and Wu, C. (2004). Interneurons of the neocortical inhibitory system. *Nat. Rev. Neurosci.* *5*, 793–807.
- McCurry, C.L., Shepherd, J.D., Tropea, D., Wang, K.H., Bear, M.F., and Sur, M. (2010). Loss of Arc renders the visual cortex impervious to the effects of sensory experience or deprivation. *Nat. Neurosci.* *13*, 450–457.
- Milosevic, I., Giovedi, S., Lou, X., Raimondi, A., Collesi, C., Shen, H., Paradise, S., O'Toole, E., Ferguson, S., Cremona, O., and De Camilli, P. (2011). Recruitment of endophilin to clathrin-coated pit necks is required for efficient vesicle uncoating after fission. *Neuron* *72*, 587–601.
- Morales, B., Choi, S.Y., and Kirkwood, A. (2002). Dark rearing alters the development of GABAergic transmission in visual cortex. *J. Neurosci.* *22*, 8084–8090.
- Okaty, B.W., Miller, M.N., Sugino, K., Hempel, C.M., and Nelson, S.B. (2009). Transcriptional and electrophysiological maturation of neocortical fast-spiking GABAergic interneurons. *J. Neurosci.* *29*, 7040–7052.
- Rougeulle, C., Glatt, H., and Lalonde, M. (1997). The Angelman syndrome candidate gene, UBE3A/E6-AP, is imprinted in brain. *Nat. Genet.* *17*, 14–15.
- Rubenstein, J.L., and Merzenich, M.M. (2003). Model of autism: increased ratio of excitation/inhibition in key neural systems. *Genes Brain Behav.* *2*, 255–267.
- Sato, M., and Stryker, M.P. (2010). Genomic imprinting of experience-dependent cortical plasticity by the ubiquitin ligase gene Ube3a. *Proc. Natl. Acad. Sci. USA* *107*, 5611–5616.
- Slepnev, V.I., and De Camilli, P. (2000). Accessory factors in clathrin-dependent synaptic vesicle endocytosis. *Nat. Rev. Neurosci.* *1*, 161–172.
- Sloviter, R.S. (1987). Decreased hippocampal inhibition and a selective loss of interneurons in experimental epilepsy. *Science* *235*, 73–76.
- Tabuchi, K., Blundell, J., Etherton, M.R., Hammer, R.E., Liu, X., Powell, C.M., and Südhof, T.C. (2007). A neuroligin-3 mutation implicated in autism increases inhibitory synaptic transmission in mice. *Science* *318*, 71–76.
- Thibert, R.L., Conant, K.D., Braun, E.K., Bruno, P., Said, R.R., Nespeca, M.P., and Thiele, E.A. (2009). Epilepsy in Angelman syndrome: a questionnaire-based assessment of the natural history and current treatment options. *Epilepsia* *50*, 2369–2376.
- Williams, C.A., Beaudet, A.L., Clayton-Smith, J., Knoll, J.H., Kyllerman, M., Laan, L.A., Magenis, R.E., Moncla, A., Schinzel, A.A., Summers, J.A., and Wagstaff, J. (2006). Angelman syndrome 2005: updated consensus for diagnostic criteria. *Am. J. Med. Genet. A* *140*, 413–418.
- Yashiro, K., Riday, T.T., Condon, K.H., Roberts, A.C., Bernardo, D.R., Prakash, R., Weinberg, R.J., Ehlers, M.D., and Philpot, B.D. (2009). Ube3a is required for experience-dependent maturation of the neocortex. *Nat. Neurosci.* *12*, 777–783.